Testing of Axially Loaded Bucket Foundation with Applied Overburden Pressure

Vaitkunaite, Evelina; Ibsen, Lars Bo; Nielsen, Benjaminn Nordahl

Publication date:
2016

Document Version
Publisher's PDF, also known as Version of record

DEPARTMENT OF CIVIL ENGINEERING
AALBORG UNIVERSITY

Testing of Axially Loaded Bucket Foundation with Applied Overburden Pressure

E. Vaitkunaite, L.B. Ibsen and B.N. Nielsen

ISSN 1901-726X
DCE Technical Report No. 209

Aalborg University
Department of Civil Engineering
Geotechnical Engineering Group

DCE Technical Report No. 209

Testing of Axially Loaded Bucket Foundation with Applied Overburden Pressure

by

E. Vaitkunaite, L.B. Ibsen and B.N. Nielsen

April 2016

Scientific Publications at the Department of Civil Engineering

Technical Reports are published for timely dissemination of research results and scientific work carried out at the Department of Civil Engineering (DCE) at Aalborg University. This medium allows publication of more detailed explanations and results than typically allowed in scientific journals.

Technical Memoranda are produced to enable the preliminary dissemination of scientific work by the personnel of the DCE where such release is deemed to be appropriate. Documents of this kind may be incomplete or temporary versions of papers—or part of continuing work. This should be kept in mind when references are given to publications of this kind.

Contract Reports are produced to report scientific work carried out under contract. Publications of this kind contain confidential matter and are reserved for the sponsors and the DCE. Therefore, Contract Reports are generally not available for public circulation.

Lecture Notes contain material produced by the lecturers at the DCE for educational purposes. This may be scientific notes, lecture books, example problems or manuals for laboratory work, or computer programs developed at the DCE.

Theses are monograms or collections of papers published to report the scientific work carried out at the DCE to obtain a degree as either PhD or Doctor of Technology. The thesis is publicly available after the defence of the degree.

Latest News is published to enable rapid communication of information about scientific work carried out at the DCE. This includes the status of research projects, developments in the laboratories, information about collaborative work and recent research results.

Published 2016 by
Aalborg University
Department of Civil Engineering
Sofiendalsvej 9-11
DK-9200 Aalborg SV, Denmark

Printed in Aalborg at Aalborg University

ISSN 1901-726X
DCE Technical Report No. 209

Contents

CHAPTER 1
Introduction

This report analyses laboratory testing data performed with a bucket foundation model subjected to axial loading. The examinations were conducted at the Geotechnical laboratory of Aalborg University. The report aims at showing and discussing the results of the static and cyclic axial loading tests on the bucket foundation model. Finally, a cyclic loading interaction diagram is given that can be applied for a full-scale bucket foundation design. For the basis, this report uses two previously published reports that contain test data and a detailed description of the test procedure:

- Vaitkunaite, E.: "Bucket Foundations under Axial Loading – Test Data Series 13.02.XX, 13.03.XX and 14.02.XX". DCE Technical Report, No. 199, Department of Civil Engineering, Aalborg University. 2015. Aalborg, Denmark.
- Vaitkunaite, E.: "Test Procedure for Axially Loaded Bucket Foundations in Sand (Large Yellow Box)". DCE Technical Memorandum, No. 51, Department of Civil Engineering, Aalborg University. 2015. Aalborg, Denmark.

1.1 Aim of the report

In a shallow offshore multi-pod foundation combination, the horizontal wind and wave loads are transferred to the axial loads and sliding. Figure 1.1 shows an example of such load transfer in the wave energy converter Wavestar. The loading conditions are also usual for offshore wind turbine foundations standing on a jacket structure.

Suction bucket foundations are shallow skirted geotechnical structures. For bucket foundations in sand, the axial tensile loading component can be critical and setting the dimensions. Senders (2009) described the failure figures for bucket foundations in sand (Figure 1.2). Constant or static tensile loading on a bucket foundations in sand results in the drained response and lowest capacity. In the offshore conditions, cyclic wind and wave loads can create long-term tensile mean loads. Such situation should be avoided based on the experiences of earlier researches (e.g. Byrne and Houlsby 2006, Kelly *et al.* 2006a).

If the loading rate is rapid enough, the pore water does not have enough time to drain

resulting in an undrained foundation behaviour. A foundation experiences high intensity loading conditions in a storm, where the structure is subjected to large cyclic wind and wave loads. The undrained tensile capacity is significantly larger than the drained capacity because of the suction pore pressure contribution to the resistance. However, such loading conditions can lead to large displacements and tilting of the overall structure (Kelly *et al.*, 2006b). Furthermore, constant cyclic tensile loading with mean tensile load and tensile cyclic amplitude can lead to irreversible upward displacements.

Model testing is an important tool that provides valuable understanding of the real

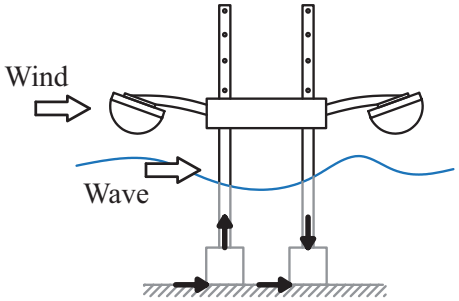

Figure 1.1 Loads on the wave energy converter Wavestar in a storm: horizontal wind and wave loads and the axial and horizontal components on a shallow foundation.

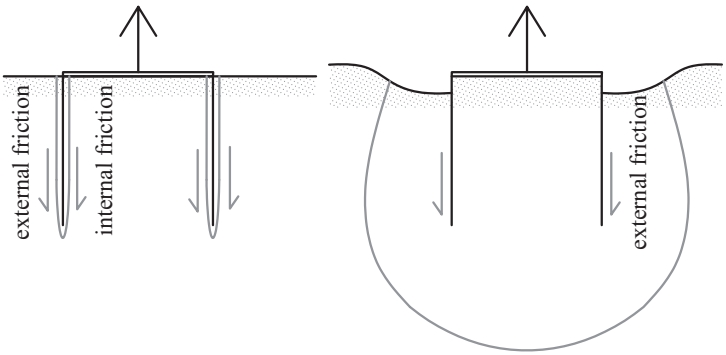

Figure 1.2 Bucket foundation tensile resistance in cohesionless soil: (left) drained response; (right) undrained response. After Senders (2009).

foundation behaviour under various loading conditions. To the knowledge of the authors, until present, no publicly available testing campaign had been performed on bucket foundations subjected to one-way tensile cyclic loading. Thus, the aim of this report is to show the axial behaviour in different effective stress levels and to set the cyclic loading interaction diagram that can be used for bucket foundation design. To fulfil the aim, a new testing facility was employed for bucket foundation testing under

axial loading. In this test set-up, an overburden pressure increased the effective stress in the soil. Consequently, the skirt friction of a bucket foundation in different soil depths could be analysed.

The selected cyclic loading program focussed on the axial loading conditions during a normal serviceability situation of an offshore structure. In such case, the foundation is subjected to long-term cyclic loading of small intensity compared to the storm case. Drained conditions are present. Therefore, the target of the testing program was the accumulated cyclic displacement and the cyclic degradation effect on the tensile capacity. The second set of tests started with slow monotonic pull-out tests that provided reference capacities. The testing program continued with the low-rate cyclic loading tests corresponding to the drained response. Finally, a post-cyclic monotonic tensile load was applied which was directly comparable to the virgin loading resistance.

CHAPTER 2
Test Set-Up

This chapter presents the principle of the overburden pressure application and provides a short overview of the test set-up facilities. The step-by-step testing procedure can be found in Vaitkunaite (2015b).

2.1 Testing rig and foundation model

Figures 2.1 and 2.2 show the testing rig and the bucket foundation model used in the testing campaign. The test set-up consisted of a large container of 2.5 m in diameter and 1.5 m height. The container was filled with 0.3 m of coarse gravel (drainage layer) and 1.2 m of Aalborg University sand No. 1. A rigid structure of four columns and beams was built to support the loading equipment which consisted of two hydraulic cylinders: installation and loading (actuator). Two displacement transducers and two load measuring cells (measuring range 250 kN) were fixed to the hydraulic cylinders.

Bucket foundation model was made of steel. It had a diameter D of 1 m, skirt length d of 0.5 m and skirt thickness t of 3 mm. The skirt was allowed to corrode naturally providing a realistic soil-structure interface. Three inner and three outer narrow pipes were fixed to the bucket foundation model. The pipes were filled with water before the installation of the foundation model to the sand. The pore pressure transducers PP were fixed on the lid and connected to the narrow pipes (Figure 2.2). They served for pore pressure measurements at different depths.

2.2 Soil properties

Aalborg University sand No.1 was used for the testing. Two reports by Hedegaard and Borup (1993) and Ibsen and Boedker (1994) contain sand classification data and triaxial testing data correspondingly. The sand properties are as follows:

- min void ratio e_{min} 0.549,
- max void ratio e_{max} 0.858,

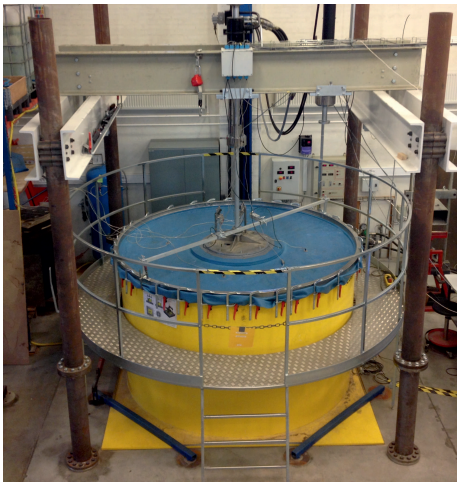

Figure 2.1 A test set-up for the axial bucket foundation testing with an applied overburden pressure.

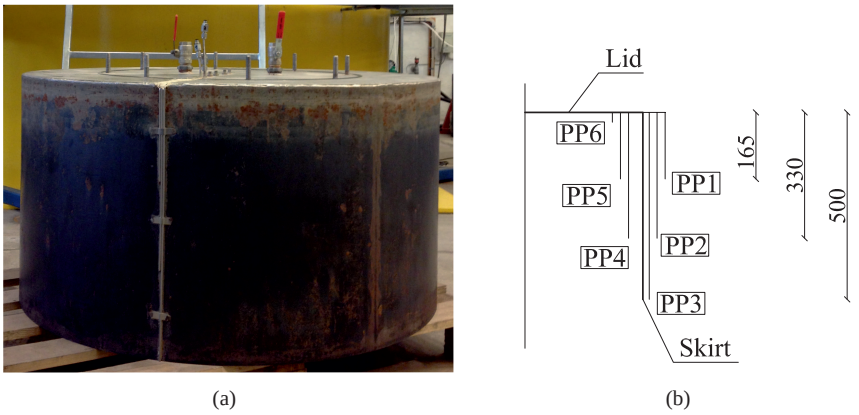

(a) (b)

Figure 2.2 (a) Bucket foundation model used in the testing campaign. (b) Positions of the points for the pore pressure measurements and labels of the pore pressure transducers PP. Distances in mm.

- specific grain density d_s 2.64 g/cm^3,
- uniformity coefficient U 1.78.

Ibsen *et al.* (2009) determined Aalborg University sand No.1 parameters for Mohr-Coulomb material. They showed that the parameters are dependent on confining pressure σ_3 and density index D_R. Results were expressed in the fitted diagrams as given in Figure 2.3. As seen, sand properties change strongly in the first 0-100 kPas confining pressure. This visualizes the typical issues related to small-scale testing in low effective stresses, such as a very high friction angle and dilation. Soil-structure inter-

face properties depend on the normal stress, relative surface roughness, soil particle shape and density. To inspect the frictional response at different soil depths, the normal stress on the bucket foundation model had to be increased. Thus, the overburden pressure was applied changing the stress conditions and providing more test results.

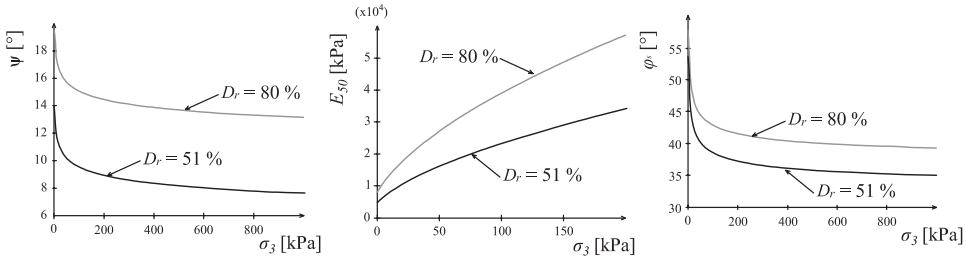

Figure 2.3 Aalborg sand No. 1 parameters dependence on the confining stress. (Ibsen *et al.*, 2009)

2.3 Test preparation

This section gives an overview of the preparation for the tests. The step-by-step testing procedure can be found in Vaitkunaite (2015b).

2.3.1 Sand preparation

Before each test, water was allowed to flow to the sand box with an upward gradient which loosened and redistributed the sand particles. The sand was compacted with a rod vibrator to the average D_R=81% (standard deviation 6%) and the effective unit weight γ'=9.4 kN/m^3. Sand density ratio was found from a laboratory cone penetration test (CPT) specially developed at Aalborg University. Larsen (2008) described the equipment and methodology behind the laboratory CPT. Ibsen *et al.* (2009) provided the empirical equation for the estimation of D_R based on cone penetration measurements. The procedure was repeated before every installation.

2.3.2 Installation

After the sand preparation, the narrow pipes on the bucket model were filled with water as mentioned in section 2.1. The bucket model was placed above the sand surface. Displacement and load transducers were zeroed and the installation started. The installation hydraulic cylinder pushed the model to the sand with a velocity of 0.2 mm/s. The two valves on the model were kept open during the installation. The installation ended with about 70 kN load F_P that consisted of 50 kN required for the installation and a small compressive pre-load of 20 kN. Due to sand dilation around the circumference of the model, the skirt was installed to approximately 490 mm depth

d_{inst}. The installation was followed by connection of the transducers and mounting of the actuator.

2.3.3 Application of the overburden pressure

A latex membrane was laid on the surface of the sand container and the bucket lid. A water pumping system was available by the sand container. Suction was applied in four points on the membrane. A filter layer prevented sand grains from being sucked into the pumping system. Suction application on the membrane evenly pressed the whole surface simulating an overburden pressure p_m. In the atmospheric pressure conditions, the pump unit could apply up to -100 kPa suction. In the testing campaign, a pressure of up to -70 kPa was aimed. In a successful test, the established level of pressure was kept constant, with only +/-2 kPa variations. The overburden pressure allowed analysing axial behaviour of the bucket foundation model in different soil depths. The following scheme in Figure 2.4 visualizes the idea of the overburden pressure application.

This method of the overburden pressure application required a very tight system

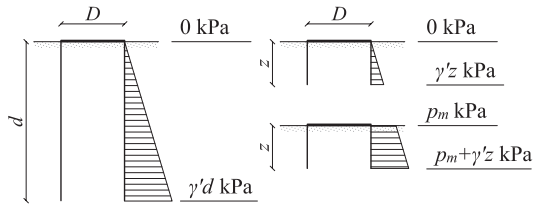

Figure 2.4 Vertical stress distribution on a bucket foundation.

and de-aired water to saturate the sand. At least 1.5 m^3 of de-aired water would have been necessary to saturate the sand which was unavailable at the time of testing. Although many attempts and special care were taken for the tightening of the system, air was present in the sand. Thus, the suction through the membrane resulted in a reduced amount of water in the sand volume that left the sand only moist. Furthermore, the sand structure has changed - the pores became larger - due to the suction method as shown in Figure 2.5. There could be two reasons for this: water cavitation or expansion due to negative pressure in the air/vapour. Despite this, the testing program continued because it was still possible to apply a constant overburden pressure and to investigate the friction response in the different soil depths. For the result analysis, soil unit weight was measured after several tests with the membrane and was found to be γ=17 kN/m^3.

After a constant membrane pressure was established, the loading could start. During tests with the overburden pressure, load, displacement and membrane pressure were measured. During tests without the overburden pressure, pore pressures were

measured too.

Figure 2.5 Sand after suction application.

CHAPTER 3
Testing program

In this report, the upward displacement, tensile load and negative pore pressure are drawn on the negative axis and marked with a negative sign.

Monotonic pull-out tests were performed with a constant velocity v of 0.002 m/s. The bucket model was pulled approximately 60 mm which was sufficient to capture the peak load F_T and the corresponding displacement w_T .

Cyclic loading tests were performed with 0.05 or 0.1 Hz frequency f. A testing program consisted of 20,000-40,000 harmonic cycles N that were followed by a post-cyclic monotonic tensile load. The post-cyclic load was applied with a displacement rate of 0.002 mm/s until the peak load F_{Pc} and the corresponding displacement w_{Pc} were measured, as shown in Figure 3.1. If the accumulated cyclic displacement w_{cyc} reached 60 mm upward displacement, the loading sequence was stopped.

Vaitkunaite (2015a) documented the tests performed in the large yellow sand box.

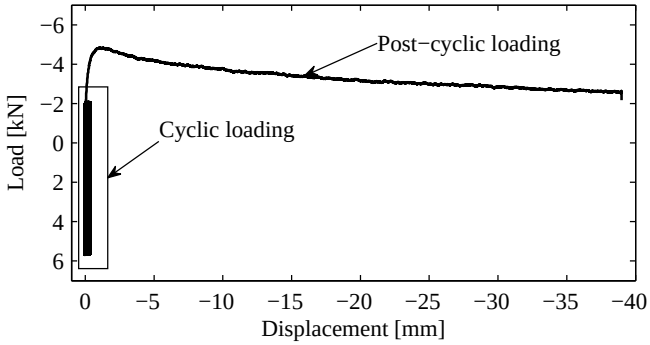

Figure 3.1 Cyclic loading with post-cyclic monotonic pull-out (test C0A0.7m0.3.2).

Tables 3.1 and 3.2 provide an overview of the performed tests. The load cell and displacement transducers were zeroed before the beginning of the loading step; thus, the tables provide only the loading response (model self-weight is zero).

Cyclic loading is described using two parameters: ξ_A and ξ_m (eqs.3.1 and 3.2). Parameter ξ_A is the ratio of cyclic loading amplitude F_{cyc} and the reference tensile load F_{TR}. The second parameter defines the ratio of the mean cyclic load F_{mean} and F_{TR}. The parameter is negative for mean tensile load, and positive for mean compressive load. In the case of perfect two-way loading, ξ_m is 0.

$$\xi_A = -\frac{F_{cyc}}{F_{TR}}, \tag{3.1}$$

$$\xi_m = -\frac{F_{mean}}{F_{TR}}. \tag{3.2}$$

Each test has an ID. For example, a monotonic loading test ID is M20.1, where M stands for monotonic, 20 for the membrane pressure aimed of 20 kPa and .1 marks the test number. A cyclic load loading test ID is, e.g. C70A0.24m-0.23, where C stands for cyclic, 70 for the aimed membrane pressure of 70 kPa, A0.24 marks the cyclic loading amplitude in the test ξ_A=0.24 and m-0.23 marks the mean cyclic load in the test ξ_m=-0.23.

Table 3.1 Summary of the monotonic loading tests.

			Loading			Installation	
p_m [kPa]	Test ID	d/D	F_T [kN]	w_T [mm]	v [mm/s]	F_P [kN]	d_{inst} [mm]
0	M0.1	0.5	-5.7	-6.3	0.001	49.6	483
0	M0.2	0.5	-6.3	-5.8	0.001	50.6	474
0	M0.3	0.5	-5.3	-4.6	0.002	49.5	473
0	M0.5	0.5	-5.9	-5.5	0.002	73.0	491
19	M20.1	0.5	-19.0	-24.3	0.001	45.3	486
21	M20.2	0.5	-15.3	-11.4	0.001	46.1	495
20	M20.3	0.5	-23.3	-7.5	0.002	57.3	487
41	M40.1	0.5	-28.2	-5.0	0.001	68.3	487
40	M40.2	0.5	-26.9	-5.2	0.002	72.8	487
73	M70.1	0.5	-96.3	-72.2	0.002	74.0	490

Table 3.2 Summary of the cyclic loading tests.

p_m [kPa]	Test ID	Cyclic loading				Post-cyclic load	
		F_{mean} [kN]	F_{cyc} [kN]	w_{cyc} [mm]	N [Hz]	F_{Pc} [kN]	w_{Pc} [mm]
0	C0A0.2m-0.4	-2.11	1.02	-0.88	39,592	-5.34	-3.83
0	C0A0.3m-0.4.1	-2.05	1.93	-1.35	38,227	-5.95	-7.60
0	C0A0.3m-0.4.2	-2.05	1.93	-6.23	39,753	-4.74	-0.53
0	C0A0.7m-0.4.1	-2.05	3.85	-63.76	8,100	-	-
0	C0A0.7m-0.4.2	-2.05	3.85	-65.80	1,285	-	-
0	C0A0.7m0.3.1	1.80	3.85	0.15	28,263	-	-
0	C0A0.7m0.3.2	1.80	3.85	0	39,980	-4.85	-1.30
0*	C0A0.4m0.3	1.91	2.30	0.04	19,629	-5.03	-3.43
0	C0A0.3m-0.1	-0.30	1.66	-0.64	39,729	(-3.49)	-8.66
0	C0A0.2m0.0	0	1.00	-0.29	40,020	-4.86	-4.84
43*	C40A0.4m0.4	11.76	11.38	0.72	19,900	-31.33	-12.35
41	C40A0.7m-0.5	-13.03	18.37	-67.55	67	-	-
41	C40A0.3m-0.7	20.12	9.33	-63.81	202	-	-
71*	C70A0.3m0.0.1	2.01	29.38	0.74	19,970	-	-
70	C70A0.3m0.0.2	1.92	29.30	1.25	40,867	-93.26	-28.29
73	C70A0.2m-0.2	-22.39	23.08	0.10	31,619	-93.90	-26.53
71	C70A0.3m-0.5	-51.67	24.49	-75.01	19,081	-	-
71	C70A0.5m-0.5	-50.61	45.78	-81.90	5	-	-
*Tests with f=0.05 Hz, other tests are with f=0.01 Hz							

CHAPTER 4
Results

This chapter provides the results of the monotonic and cyclic loading tests. It includes the main results of the load, displacement and stiffness responses. Finally, the chapter presentes a cyclic loading interaction diagram applicable to bucket foundation design in dense sand.

4.1 Monotonic tensile loading tests

Monotonic tensile loading tests were performed at the overburden pressure levels of 0, 20, 40 and 70 kPa. The average membrane pressure level p_m varied +/-2 kPa as seen in Table 3.1. The four tests with overburden pressure of 0 kPa showed very similar response. Three tests were formed with 20 kPa overburden pressure and showed a bit scattered peak tensile load results. M40 tests were aborted after a displacement of only -8 mm both times due to cracks in the membrane and a sudden pressure loss. However, the peak load was captured and recorded. Only one monotonic tensile loading with 70 kPa was successful. Other attempts failed due to the loss of pressure or other technical issues. As seen in Figure 4.1, in most of the cases F_T was reached at the upward displacement of up to -10 mm ($0.01D$) except two tests, M20.1 and M70.1 (correspondingly, $0.02D$ and $0.07D$).

The development of peak tensile resistance compared to the corresponding displacement was visualized by the corresponding peak stiffness k_{peak}. It is used as a sort of normalization for comparison of the resistance development in different tests. Figure 4.2 shows k_{peak} values at different surcharge levels. As the tests with the overburden pressure had different soil unit weights (see sections 2.3.1 and 2.3.3), the surcharge was estimated at the middle of the skirt depth $d/2$. This quantified better the tests with different overburden pressures. Seven k_{peak} values at p_m of 0, 20 and 70 kPa lied around 1 MN/m while the other three tests showed higher stiffness.

As expected, different levels of unit skirt friction f_s were developed in the monotonic loading tests. The skirt friction corresponds to the measured tensile load divided by the sum of the inner and outer areas of the skirt in contact to the soil. According to the testing data, a quadratic fitting resembled best the measured tensile capacities at the different surcharge levels (Figure 4.3) which is worth taking a little closer look

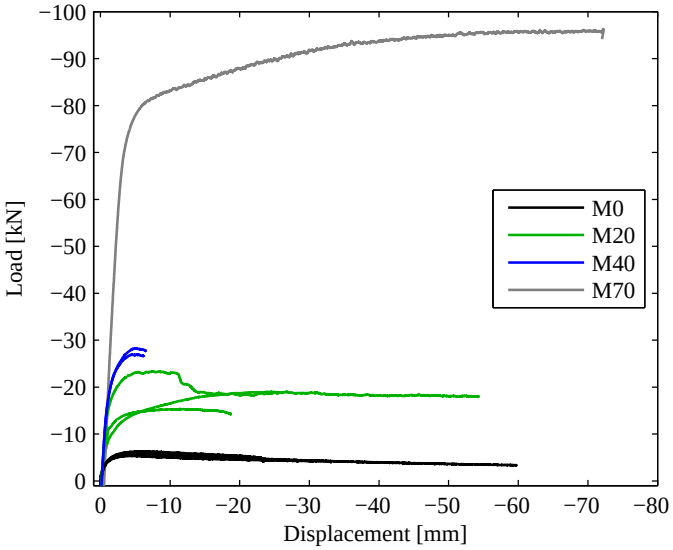

Figure 4.1 Monotonic tensile load vs. displacement for tests with 0, 20, 40 and 70 kPa overburden pressure.

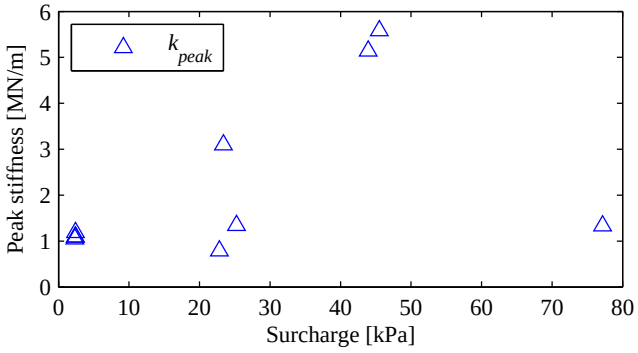

Figure 4.2 Peak stiffness at different overburden pressure levels.

into. Unit skirt friction f_s can be estimated using a well known equation 4.1 that depends on the effective vertical stress σ'_v, lateral earth pressure coefficient K and interface friction angle δ as follows:

$$f_s = \sigma'_v K tan\delta, \tag{4.1}$$

Obviously, σ'_v increases linearly with depth for a uniform soil layer. Byrne and Houlsby (2002) used $Ktan\delta$=0.5 for back-calculations of different scale model tests

and showed that it is a well applicable value for bucket foundations. Knowing this, the data in Figure 4.3 should have had a linear fit. Gaydadzhiew *et al.* (2015) investigated Aalborg University sand No. 1 properties in the same sand container as used in this testing program. They used a Marchetti dilatometer (DMT) for the examination of horizontal stress and K values. The lateral pressure coefficients were rather scattered between approximately 0.4 and 4.5 for vertical effective stress between 3 and 9 kPa. The mean value of K was approximately 1.6. However, the testing program was limited to rather few attempts. Boulon and Foray (1986) showed that K value decreases to a constant value together with the increasing confining pressure as seen in Figure 4.4. Thus, an attempt was taken to back-calculate the lateral earth pressure value using equation 4.1 and assuming that δ is constant and equal to 29°, see Figure 4.5. The back-calculated K value has a similar tendency of changing depending on the stress conditions as seen in Figure 4.4. At the surcharge of 6 kPa, lateral earth pressure coefficient lies approximately at about 1.8 which is close to 1.6 estimated by Gaydadzhiew *et al.* (2015).

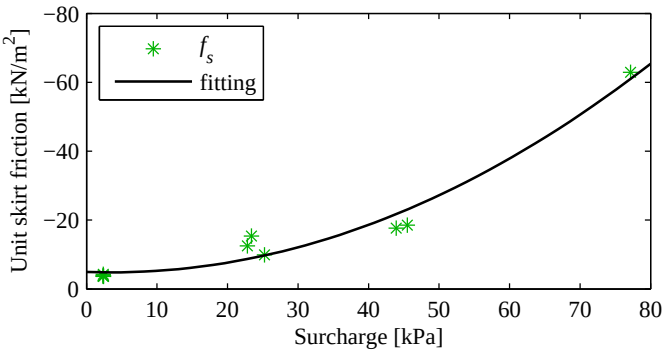

Figure 4.3 Peak tensile load developed at different surcharge levels.

4.2 Cyclic loading tests

Cyclic loading conditions were modelled taking into consideration the monotonic load results. For each of the overburden pressure levels, the reference monotonic tensile resistance F_{TR} was estimated as the average of the peak tensile resistances F_T. The intention was to test different levels of mean cyclic load and amplitudes and to find the most critical load case. All of the cyclic tests were exposed to peak tensile loads, but the mean loads were various: small compressive, zero (perfect two-way loading) or tensile load. Most of the tests proved to be in a "stable zone". This means that during the whole cyclic loading sequence of 20,000-40,000 cycles, the vertical displacement was close to zero ($|w_{cyc}|$<0.01D). Figure 4.6 shows some typical examples of this behaviour.

However, as seen in Table 3.2, five cyclic loading tests were aborted during the cyclic

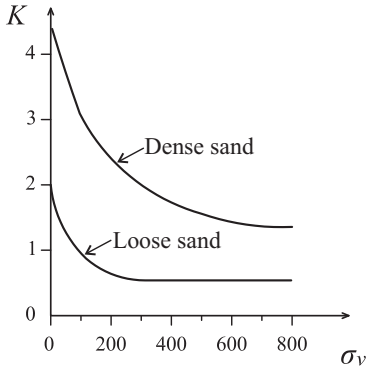

Figure 4.4 Lateral earth pressure vs. confining pressure. Reproduced from the figure presented by Boulon and Foray (1986)

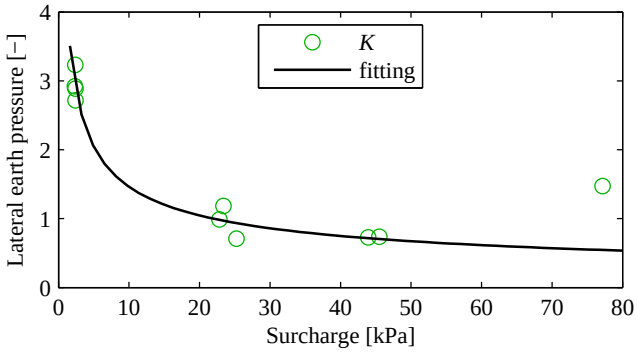

Figure 4.5 Back-calculated lateral earth pressure vs. confining pressure.

loading because the upward cyclic developed rapidly and reached the limit of about 65 mm. Figure 4.7 shows four of those tests. In all cases, critical tensile loading was applied, where the peak loads reached or even succeeded the reference tensile loads F_{TR}. It was noticed that even under so critical loads, the tests without the overburden pressure and with saturated sand could hold longer than the tests with p_m>0. The reason for this was the development of pore suction that could help the bucket model resist the critical loading. For example, Figure 4.8 shows full cyclic loading data for test C0A0.7m-0.4.2. The inner pore pressure transducers (PP4-PP6) measured a small negative suction that at the last part of the cyclic loading reached -8 kPa suction under the bucket model lid. This suction divided by the inner area of the lid provides a resistance suction force of 10 kN which is larger than the peak tensile load applied of -5.9 kN. Even though the loading frequency was low (0.1 Hz), it was sufficient to create partial drainage conditions and generate negative pore suction in the tests with the critical loading.

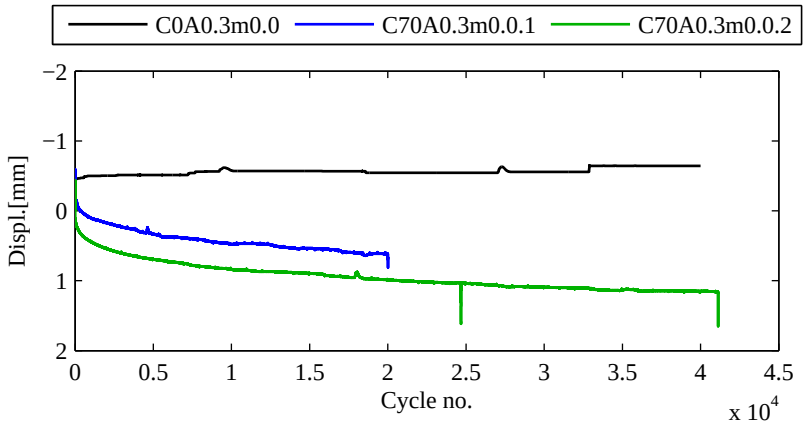

Figure 4.6 Accumulated displacement vs. cycle number for three tests.

Eight cyclic loading tests ended up with a post-cyclic monotonic pull-out F_{Pc}. Fig-

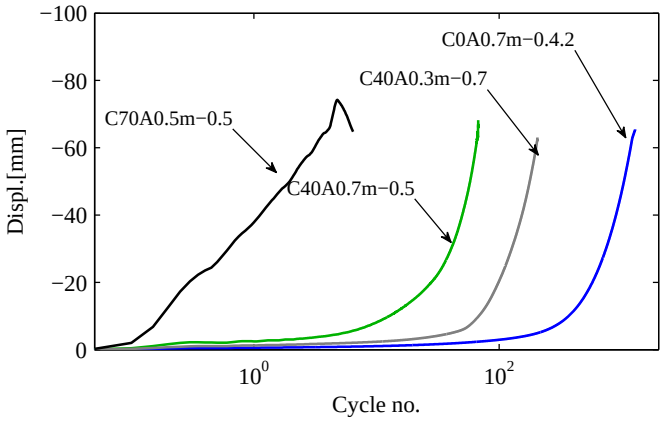

Figure 4.7 Accumulated displacement vs. cycle number for four tests where the displacement was developed in less than 20,000 cycles.

ures 4.9, 4.10 and 4.11 show the results from tests with different overburden pressures. Virgin monotonic peak load F_T is marked at the corresponding displacement w_T. F_{Pc} values were up to 15% lower than F_T in the tests with 0 kPa overburden pressure (Figure 4.9). Very few successful tests with the post-cyclic loading were performed in tests with the overburden pressure of 40 and 70 kPa. Out from those few, it seems that no obvious cyclic degradation was present after the long-term cyclic loading.

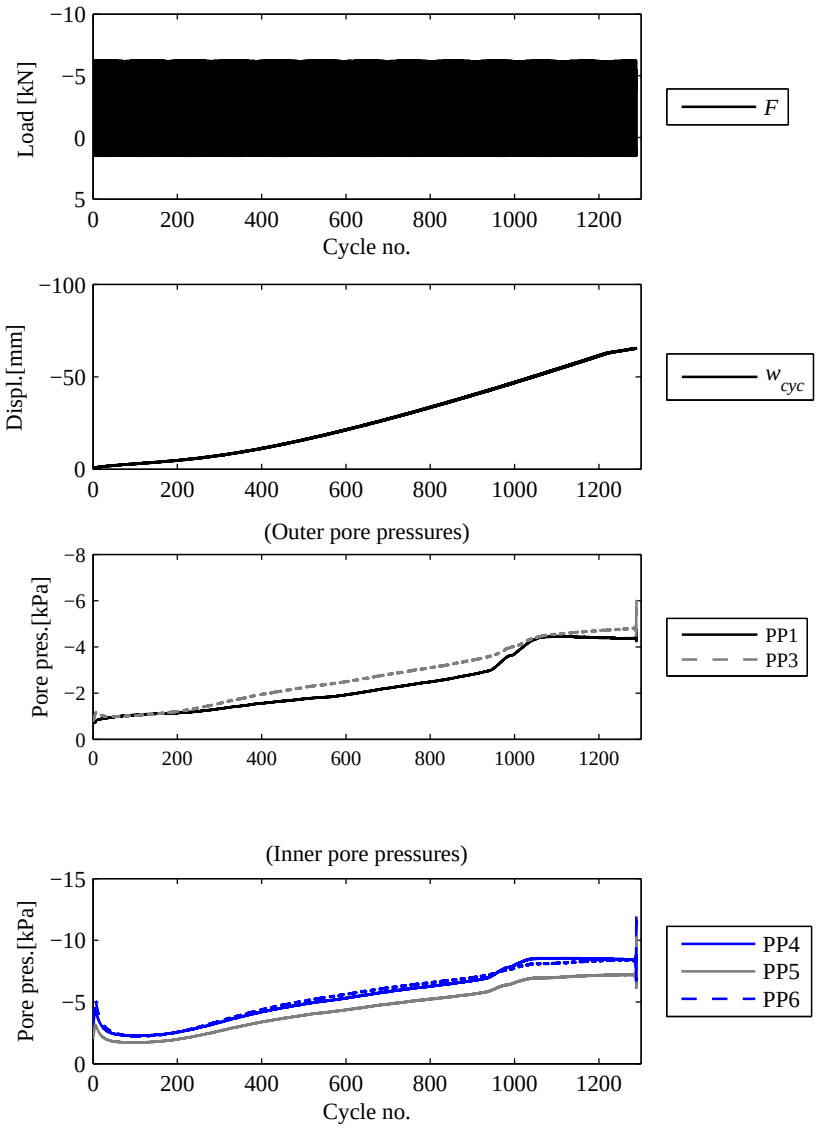

Figure 4.8 Full data for the cyclic loading test C0A0.7m-0.4.2.

Table 4.1 shows stiffness results for cyclic loading tests. The following ratios of

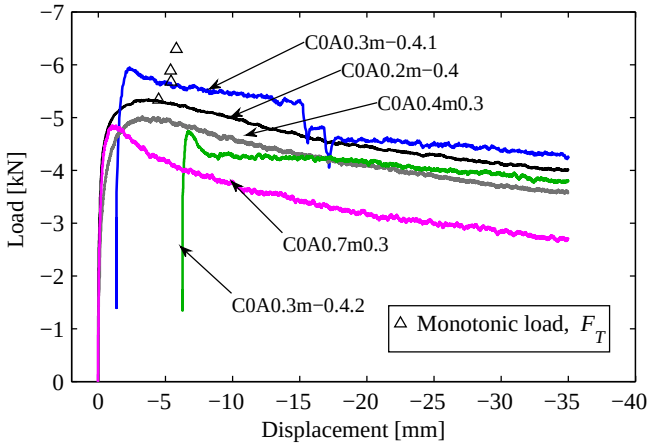

Figure 4.9 Post-cyclic tensile loading for two tests vs. vertical displacement for tests with 0 kPa overburden pressure. Triangle marks the peak monotonic tensile load.

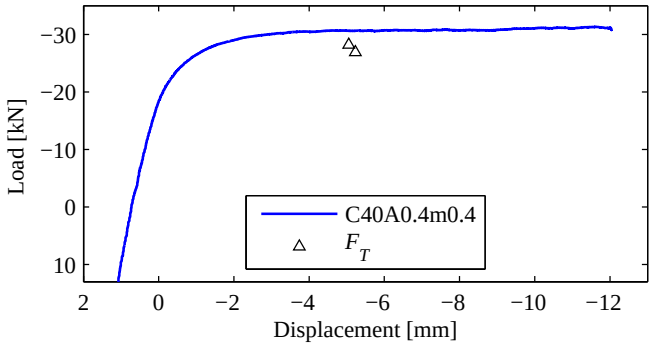

Figure 4.10 Post-cyclic tensile loading for two tests vs. vertical displacement for tests with 40 kPa overburden pressure. Triangle marks the peak monotonic tensile load.

load and displacement were considered: cyclic unloading stiffness k_{UN} where the trough value was subtracted from the peak value of a cycle, cyclic loading stiffness k where the peak value was subtracted from the trough value of a cycle and peak stiffness k_{Pc} for the post-cyclic monotonic loading part. Three tests developed very small cyclic displacement and had very scattered and extremely high stiffness values, they are marked with a star in Table 4.1. Overall, cyclic stiffness was always significantly higher than the virgin loading stiffness k_{peak} (see section 4.1). By its magnitude, cyclic unloading stiffness was very similar to the loading stiffness except three tests where k_{UN} was higher than k. The post-cyclic peak stiffness k_{Pc} was generally higher than k_{peak} with the mean value of 2.1 MN/m.

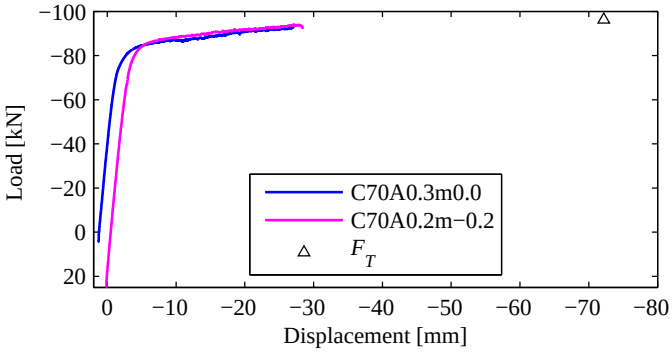

Figure 4.11 Post-cyclic tensile loading for two tests vs. vertical displacement. Triangle marks the peak monotonic tensile load.

Finally, based on the testing data, a cyclic loading interaction diagram was prepared.

Table 4.1 Stiffness results for cyclic loading tests.

p_m, [kPa]	Test ID	k_{UN}, [MN/m]	σ, [MN/m]	k, [MN/m]	σ, [MN/m]	k_{Pc}, [MN/m]
0	C0A0.2m-0.4	-	-	-	-	1.4
0	C0A0.3m-0.4.1	-	-	-	-	2.6
0	C0A0.3m-0.4.2*	1781	929.1	1705	892	0.7
0	C0A0.7m-0.4.2	21.34	8.68	19.08	7.938	-
0	C0A0.7m0.3.2	228.9	42.0	228.8	42.4	3.7
0	C0A0.4m0.3*	3190	717.9	3150	677.1	1.5
0	C0A0.2m0.0*	5469	2011	5704	2451	-
43	C40A0.4m0.4	17.1	0.5	17.1	0.5	2.7
41	C40A0.7m-0.5	8.8	3.7	7.3	2.9	-
41	C40A0.3m-0.7	183.6	157.2	39.4	5.4	-
71	C70A0.3m0.0.1	39.7	0.3	39.7	0.3	-
70	C70A0.3m0.0.2	41.2	0.4	41.2	0.4	-
73	C70A0.2m-0.2	39.2	0.5	39.2	0.5	-
71	C70A0.3m-0.5	34.8	1.0	34.8	1.0	-
71	C70A0.5m-0.5	13.0	5.5	5.5	0.9	-
*Rough estimate						

Figure 4.12 shows the results of cyclic loading that led to maximum -50 mm ($0.05D$) upward displacement w_{cyc}. The normalized cyclic amplitude ξ_A and mean load ξ_m were used as the main input to the diagram. The diagram was divided into two zones: stable and unstable. The stable zone contains most of the performed tests, because the displacement developed was close to zero. The response was completely drained in these tests. In the stable zone, a bucket foundation would resist the tensile loading without an excessive upward displacement. As seen, a small mean tensile load of up

to ξ_m=-0.5 can be allowed for the design. All the tests in the unstable zone resulted in a gradual pull-out of the bucket model. In this case, the foundation would need extra ballast or to be increased in size.

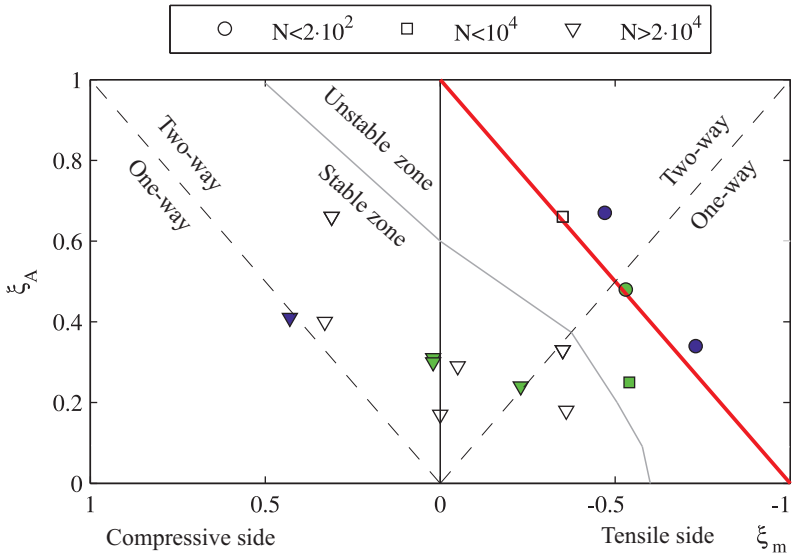

Figure 4.12 Interaction diagram for the cyclic loading tests with overburden pressure: 0 kPa (empty marks), 40 kPa (blue) and 70 kPa (green). The red line marks the limit for the drained tensile capacity.

CHAPTER 5
Conclusion and Recommendations

Conservative assumptions often govern bucket foundation design in sand. Several earlier researchers also recommended that no tensile loading should be allowed for a safe design. But there are no publicly available studies that have focussed on the cyclic behaviour of a bucket foundation subjected to one-way tensile loading. Consequently, this study took a closer look into the cyclic tensile loading on a bucket foundation model. The drained cyclic response was examined simulating the long-term cyclic loading conditions for an offshore structure under the normal serviceability performance. Cyclic degradation was tested applying post-cyclic pull-out loads on the bucket foundation model. The physical model analysis led to the following observations:

- Unit skin friction increased with the increasing overburden pressure. Interestingly, the measured increase was non-linear which could be explained by a changeable lateral earth pressure coefficient.

- In terms of stiffness, cyclic loading stiffness was much higher than the virgin monotonic loading stiffness. Post-cyclic monotonic loading stiffness was approximately twice larger than the virgin monotonic loading stiffness. However, cyclic unloading and loading stiffnesses were very similar.

- In most of the performed cyclic loading tests, the sand could freely drain and no pore pressure was built up. It was found that mean tensile loads can be allowed for long-term loading for ξ_m up to -0.5. For the long-term loading analysis, the tensile drained capacity should never be exceeded, because it would lead to pull-out.

- After long-term cyclic loading, cyclic degradation of up to 15 % was noticed in tests with 0 kPa overburden pressure. Only a few tests with 40 and 70 kPa

overburden pressure succeeded, and they showed no cyclic degradation. But more tests are needed to confirm a tendency.

Interface properties were analysed based on the testing data. Variation of the properties, such as different skirt roughness and other types of sand, would provide more information that could be used for a more detailed interface parameter analysis. Moreover, better knowledge about the lateral earth pressure would be very useful and clarifying the soil conditions. Dilatometer seems to be a suitable tool for the horizontal stress analysis.

The interaction diagram is valid only for a bucket foundation with d/D=0.5. Different shapes of foundation model should be tested to provide more data. Rather few tests were successful when testing the post-cyclic monotonic loading with the applied overburden pressure. More tests would provide a better overview of the results and reduce the scatter in the data.

CHAPTER 6
List of Symbols

Greek Symbols

γ	Total soil unit weight
γ'	Effective soil unit weight
δ	Soil-structure interface friction angle
ξ_A	Ratio of cyclic loading amplitude and static resistance
ξ_m	Ratio of mean cyclic load and static resistance
σ_3	Confining pressure
σ_v	Vertical stress
σ'_v	Effective vertical stress
φ_s	Secant friction angle
Ψ	Dilation angle

Latin Symbols

D	Bucket model diameter
D_R	Relative soil density
$E_{\bar{5}0}$	Secant Young's modulus
F	Load
F_{cyc}	Cyclic load amplitude
F_{mean}	Mean cyclic load
F_P	Preload during installation
F_{Pc}	Peak post-cyclic tensile load

F_T	Peak tensile load
F_{TR}	Reference tensile load (average of F_T)
K	Lateral earth pressure coefficient
N	Cycle number
PP	Pore pressure transducer
U	Uniformity coefficient
d	Skirt length
d_{inst}	Installed skirt length
d_s	Specific grain density
e_{max}	Maximum void ratio
e_{min}	Minimum void ratio
f_s	Unit skin friction
f	Loading frequency
k	Cyclic loading stiffness
k_{Pc}	Post-cyclic monotonic loading stiffness
k_{peak}	Monotonic loading stiffness
k_{UN}	Cyclic unloading stiffness
p_m	Membrane pressure
p_t	Tank pressure
v	Tensile load velocity (Pull-out rate)
t	Skirt thickness
w_{cyc}	Displacement during cyclic load
w_T	Displacement at peak tensile load
w_{Pc}	Displacement at peak post-cyclic tensile load

Bibliography

Boulon, M. and Foray, P. (1986). Physical and numerical simulations of lateral shaft friction along offshore piles in sand. *Proceedings of the Third Int. Conf. On Numerical Methods in offshore piling, Nantes.*, 127–147.

Byrne, B.W. and Houlsby, G.T. (2002). Experimental investigations of response of suction caissons to transient vertical loading. *Journal of Geotechnical and Geoenvironmental Engineering* **128(11)**, 926–939.

Byrne, B.W. and Houlsby, G.T. (2006). Assessing novel foundation options for offshore wind turbines. *Proceedings of World Maritime Technology Conference, London*.

Gaydadzhiew, D.T., Puscasu, I., Vaitkunaite, E., and Ibsen, L.B. (2015). Investigation of dense sand properties in shallow depth using cpt and dmt. *Proceedings of the Third International Conference on the Flat Dilatometer* **132**, 223–230.

Hedegaard, J. and Borup, M. (1993). *Klassifikationsforsoeg med Baskard Sand No. 15*. Department of Civil Engineering, Aalborg University, Aalborg.

Ibsen, L.B. and Boedker, L. (1994). *Baskarp Sand No. 15: data report 9301*. Department of Civil Engineering, Aalborg University, Aalborg.

Ibsen, L.B., Hanson, M., Hjort, T., and Thaarup, M. (2009). Mc-parameter calibration of baskarp sand no.15. pp. 16.

Kelly, R.B., Houlsby, G.T., and Byrne, B.W. (2006a). A comparison of field and laboratory tests of caisson foundations in sand and clay. *Géotechnique* **56(9)**, 617–626.

Kelly, R.B., Houlsby, G.T., and Byrne, B.W. (2006b). Transient vertical loading of model suction caissons in a pressure chamber. *Géotechnique* **56(10)**, 665–675.

Larsen, K.A. (2008). *Static Behaviour of Bucket Foundations: Thesis submitted for the degree of Doctor of Philosophy.* DCE Thesis; Nr. 7, vol. 1. Department of Civil Engineering, Aalborg University, Aalborg.

Senders, M. (2009). *Suction caissons in sand as tripod foundations for offshore wind turbines*. PhD Thesis, University of Western Australia.

Vaitkunaite, E. (2015a). *Bucket Foundations under Axial Loading: Test Data Series 13.02.XX, 13.03.XX and 14.02.XX*. Department of Civil Engineering, Aalborg University, Denmark. DCE Technical Reports no. 199, ISSN (print) 1901-726X.

Vaitkunaite, E. (2015b). *Test Procedure for Axially Loaded Bucket Foundations in Sand (Large Yellow Box)*. Department of Civil Engineering, Aalborg University, Denmark. DCE Technical Memorandum no. 51, ISSN 1901-7278.

Recent publications in the DCE Technical Report Series

ISSN 1901-726X
DCE Technical Report No. 209